Thermochimica Acta, 75 (1984) 219–232
Elsevier Science Publishers B.V., Amsterdam – Printed in The Netherlands

DESCRIPTIVE OXIDATIVE PROFILES FOR PYRITE IN THE LOW TEMPERATURE ASH COMPONENT OF COALS BY DIFFERENTIAL THERMAL ANALYSIS

C.M. EARNEST

Perkin-Elmer Corporation, Main Avenue, M/S 131, Norwalk, CT 06856 (U.S.A.)

(Received 21 November 1983)

ABSTRACT

Experiments leading to the DTA oxidative thermal curves for pyrite, marcasite, and several low temperature ash (LTA) specimens of coals were performed. The coal seams represented by the LTA specimens were the Herrin 6 seam (southwestern Illinois), Hazard 7 seam (eastern Kentucky) and the Hazard 8 seam (eastern Kentucky). Synthetic mixtures containing pyrite, ferrous sulfate monohydrate, and alumina were also studied to determine the effect of iron(II) sulfates on the DTA oxidative profiles. The effects of sample size and sample distribution in the DTA sample cup of natural pyrite and marcasite specimens on the observed thermal curve were also studied. Similarly, the variation of the oxidative thermal curves with pyrite level in the LTA specimens was observed. Distinguishing features of the thermal curves for the LTA specimens obtained in dynamic air purge are also identified and discussed.

INTRODUCTION

Pyrite (FeS_2) is the major inorganic sulfur compound found in coals. Pyrite is of special interest from an environmental standpoint since its combustion leads to the production of sulfur dioxide gas. The $Fe_2O_3(s)$ product of oxidation contributes to the ash material along with combined $SO_X(g)$ with existing CaO(s) in the ash. The amount of iron and its oxidation state influence the ash fusion temperature. Deposits of $Fe_2O_3(s)$ have been reported on the superheating and waterwall surfaces of power plants and are attributed to the pyrite content of the fossil fuel being burned.

In the course of a detailed thermal analysis study dealing with low temperature ash (LTA) components of several pyrite containing coals from southwestern Illinois and eastern Kentucky, it was observed that the thermal analysis peaks obtained by differential thermal analysis (DTA), thermogravimetry (TG), and derivative thermogravimetry (DTG) were, in many cases, either altered or shifted when compared to those exhibited by the individual minerals themselves. In the following study, some sample hand-

0040-6031/84/$03.00

ling techniques, synthetic mineral mixtures, and low temperature ash materials are investigated in an attempt to explain these phenomena.

EXPERIMENTAL

The major pyrite ore used in this study was obtained from the mineralogical collection of Drs. O. Katkins and William Bryce, Department of Geology, University of Pittsburgh at Johnstown (UPJ), Johnstown, Pennsylvania. A second pyrite specimen was purchased from Wards Natural Science Establishment, Inc., Rochester, NY. This specimen was received in the form of 0.5-in. cubes and was originally collected at Navajun, Logrono, Spain. Both the UPJ and Spanish specimens were subjected to careful mechanical grinding prior to use. With the exception of the comparative oxidative profiles given in Fig. 2 of this work, the UPJ specimen was used for all studies which follow.

A high purity marcasite specimen (Missouri, U.S.A.) which was obtained from F.L. Fiene, Institute for Mining and Mineral Resources (IMMR), University of Kentucky, Lexington, Kentucky, was also used in this study. Although not shown in the thermal curves of this work, an Australian marcasite specimen was obtained from the Geology Department, J.C. Cook University, Townsville, Queensland. This specimen was originally collected at the Kuridala Copper Mine 30 miles south of Cloncurry, Queensland. The low temperature ash specimens of several coals used in this study were obtained from the IMMR, University of Kentucky. The temperature ashers used include an LFE Model LTA-504 and International Plazma Company Models PM108C and PM101C. In each asher an oxygen flow of 150–200 $cm^3\ min^{-1}$ and an RF power of 30–40 W per chamber was employed. All pyrite estimates given for the LTA specimens in this work were made using a Philips Model 3100 X-Ray Diffractometer located at IMMR. This XRD unit employed a Cu K_α radiation source and was equipped with a graphite monochrometer and automatic divergence slit.

All DTA thermal curves reported in this work were obtained using a Perkin-Elmer microcomputer-based DTA-1700 High Temperature Differential Thermal Analysis System. Only the DTA mode of operation of this instrument was used in the studies presented here. In this case, the linearized ΔT (temperature difference) signal between two Pt/Pt–10% Rh thermocouples was displayed as the ordinate signal on either a Perkin-Elmer XY_1Y_2 Recorder or the Perkin-Elmer Thermal Analysis Data Station. In all cases, the linearized sample thermocouple temperature was displayed on the abscissa of the DTA thermal curve. The temperature axis was calibrated using ICTA certified reference quartz (SRM 760) which was obtained from the U.S. National Bureau of Standards, Washington, DC. Ceramic liners were used in the DTA sample holder cup. It was found that platinum liners could

also be used with small pyrite samples and for all LTA specimens of this study in dynamic air atmospheres. In these cases, the pyrite oxidation is complete prior to the decomposition temperature for pyrite.

All results of thermogravimetry presented in this study were obtained with a Perkin-Elmer TGS-2 Thermogravimetric Analysis System used in conjunction with a System 4 Microcomputer Controller and Perkin-Elmer XY_1Y_2 Potentiometric Recorder. The DTG thermal curve was obtained simultaneously with the TG thermal curve using a Perkin-Elmer FDC-1 First Derivative Computer. All sulfur analyses reported in this work were performed using a Perkin-Elmer Model 240C Elemental Analyzer in the sulfur analysis mode of operation. A Perkin-Elmer Model 240DS Data Station was used with the elemental analyzer.

RESULTS AND DISCUSSION

The mechanism of the oxidation of pyrite in air has been the subject of much study and speculation [1–13]. Thermal analysis data on the oxidation of sulfides, in general, is somewhat inconsistent. As pointed out by a number of workers [8,11,13], the factors which seem to be important in such studies are good air circulation in the analyzer cell, constant experimental conditions, and small sample size. Kopp and Kerr [11] have reported that oxidative peak temperatures are lowered with decreasing particle size.

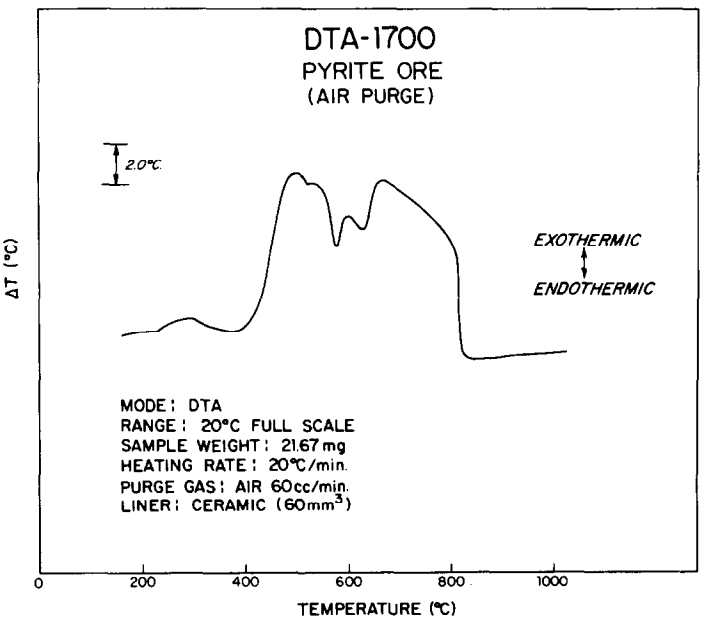

Fig. 1. DTA oxidative thermal curve for a 21.67-mg sample of pyrite. Undiluted specimen obtained at a heating rate of 20°C min^{-1}.

Figure 1 shows the DTA curve for a 21.67 mg sample pyrite specimen of this study in dynamic air purge. Oxidative thermal curves of this type have been reported for many years. It was the multistep nature of this broad range (ca. 365–800°C) oxidative curve which led researchers to offer both speculative and experimental evidence for explaining this phenomenon. There are basically two explanations which were offered. The first, is that given by Mackenzie [1] a number of years ago. In this case, localized oxygen depletion followed by surging replenishment of oxidant was believed to cause the multi-exo/endo thermal curve. The second explanation is that the pyrite goes through an intermediate oxidative step to ferrous sulfate ($FeSO_4$) as it progresses to the final oxidation products of $Fe_2O_3(s)$ and $SO_2(g)$. Thus, some of the endothermic behavior within the broad exothermic profile is believed to be due to the decomposition of iron sulfates. Banerjee [4] reported the results of a study involving DTA, TG, and DTG of a synthetic FeS_2 sample in a dynamic air atmosphere. His results indicate that the formation of $FeSO_4(s)$, interaction of pyrite with $FeSO_4$, direct oxidation of pyrite to $Fe_2O_3(s)$, and decomposition of iron sulfates can all take place during the oxidative sequence for pyrite. Banerjee supported much of his mechanistic conclusions with X-ray diffraction data.

Figure 2 shows the resulting oxidative thermal curves which were obtained

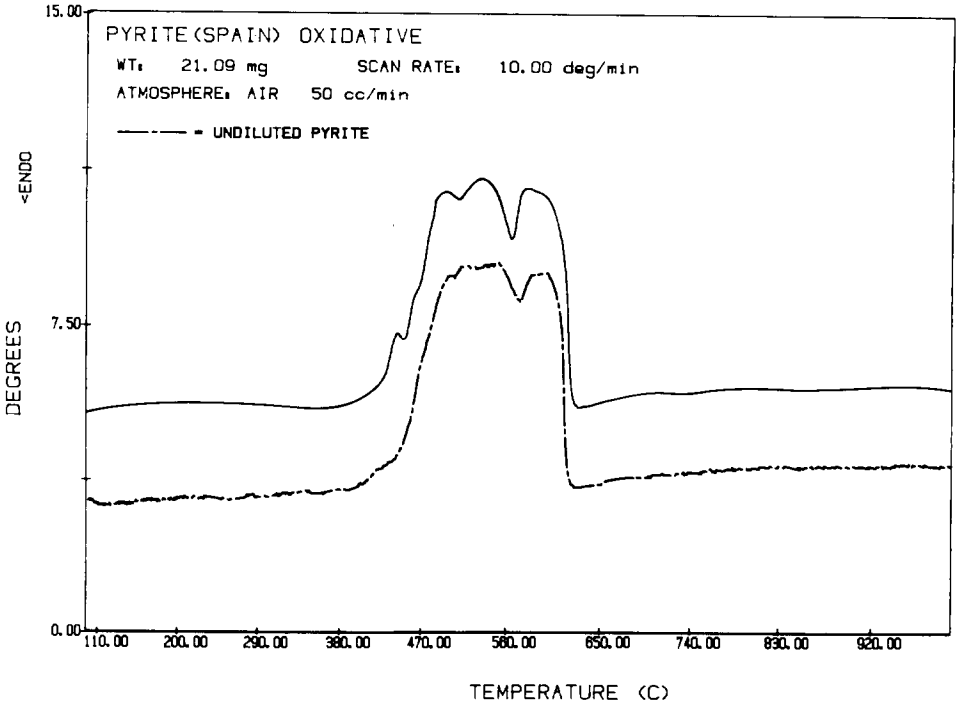

Fig. 2. DTA oxidative thermal curves for two undiluted pyrite specimens obtained at a heating rate of 10°C min^{-1}. Upper curve: 21.09 mg Spanish specimen; lower curve: 19.92 mg of UPJ specimen.

when the heating rate was reduced to 10°C min^{-1} for both the UPJ and Spanish pyrite specimens. In this case, both the sample size and sample handling technique (undiluted specimen) are the same as that for the thermal curve given in Fig. 1. On comparing Figs. 1 and 2, it can be seen that the temperature range of the exothermic oxidation of the pyrite is reduced by approximately 200°C. The temperature of initiation in this case ca. 360°C and the extrapolated onset temperature for the major exothermic portion of the thermal curve was 440.5°C. Both specimens exhibit similar endothermic activity within the oxidative profile. The major endothermic dip in both thermal curves is near 570°C.

Mackenzie [1] has shown that if the sample size is reduced, the broad multistep exotherm may be reduced to a singular exothermic peak. This observation is in line with the surging oxygen depletion/replenishment theory. Figure 3 shows the thermal curve for the UPJ pyrite specimen of this study when the sample size is reduced to 6.06 mg. This specimen, other than being smaller in sample size, was analyzed in the same fashion as that in Fig. 2. The broad exothermic oxidative profile is further reduced to a total range of ca. 134°C and the oxidation is complete by 575°C.

Pyrite / Al_2O_3 mixture

In all cases shown in Figs. 1, 2 and 3, the pyrite is resting in one continuous pile at the bottom of the ceramic liner with no diluent used in the sample specimen. In using such oxidative profiles for the recognition of pyrite in low temperature ash specimens or naturally occurring species, it

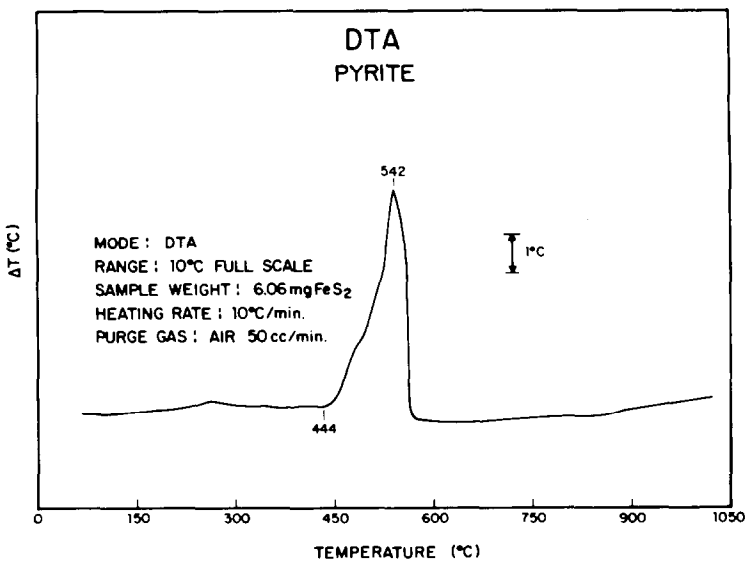

Fig. 3. DTA oxidative thermal curve for an undiluted 6.06-mg sample of pyrite.

must be noted that the FeS_2 component will be somewhat randomly distributed throughout the volume of the sample used (60 mm^3 liner in this case). Therefore, the air availability would be increased when the sulfide mineral is distributed in such a fashion and the chance of an oxygen depletion/replenishment surging profile would be minimized.

To test this hypothesis, another sample of the pyrite was studied by DTA in dynamic air purge. In this case, the pyrite was thoroughly mixed with Al_2O_3 diluent prior to placing it in the DTA liner cup. This is believed to be closest to the distributive situation which is represented by pyrite in a low temperature coal ash specimen in the DTA sample liner cup. The total mass of pyrite contained in this mixture was 4.15 mg. Figure 4 shows the resulting DTA curve for the pyrite/Al_2O_3 mixture. The oxidative profile is further reduced and a sharp peak maximum is observed at 547°C. This behavior is essentially the same as that given by Bollin [8] for the oxidative profile and peak maximum for pyrite.

Figure 5 gives the TG/DTG curve for a 10.57 mg sample of a similar pyrite/Al_2O_3 mixture. The total mass of pyrite ore represented by this TG sample is 2.44 mg. One notes the close similarity of the DTG curve in Fig. 5 with the DTA curve of Fig. 4. In terms of stoichiometric relations in the TG curves, the following expression is given for complete oxidation of the pyrite:

$$4\ FeS_2(s) + 11\ O_2(g) \rightarrow 2\ Fe_2O_3(s) + 8\ SO_2(g)$$

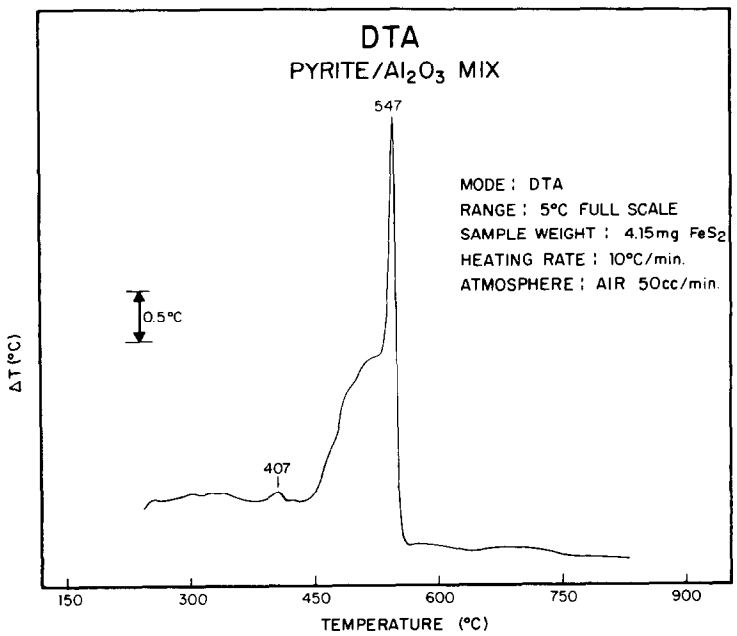

Fig. 4. DTA oxidative thermal curve for a pyrite/Al_2O_3 mixture containing 4.15 mg of pyrite.

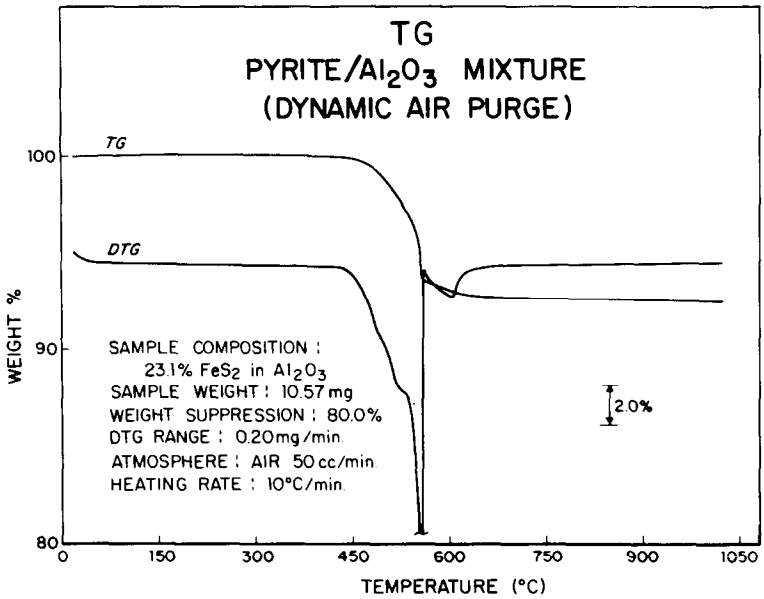

Fig. 5. TG–DTG oxidative thermal curve for a pyrite/Al_2O_3 mixture.

When four gram moles of FeS_2(s) are converted to two gram moles of Fe_2O_3 the percentage weight loss is 33.44%. The pyrite ore specimen of this study was observed to lose only 32.4% of its original mass upon oxidation which is 96.9% of the theoretical value for complete oxidation of a pure FeS_2 specimen.

Marcasite in Al_2O_3

There are actually two forms of FeS_2 which may be present in coals. Pyrite is the cubic modification and marcasite is an orthorhombic form. Marcasite is often referred to as the low temperature form. Of the two, pyrite is by far the most common and most abundant in the mineral matter of coals.

In this study, two marcasite specimens were studied in the same fashion as the pyrite specimens in dynamic air atmosphere. Essentially the same oxidative profiles were observed for the marcasite specimens as were observed with the pyrite for the particular experimental conditions. The major difference between the oxidative thermal curves is that the sharp exothermic peak observed for the FeS_2/Al_2O_3 mixture was found, on average, to be 25°C lower for the marcasite specimens than for the pyrite specimen of this study. This can be observed by comparing the DTA curves in Figs. 4 and 6.

Low temperature ash specimens

The oxidative profiles for the pyrite component of low temperature ash materials from coals are somewhat different from those given in Figs. 1–5.

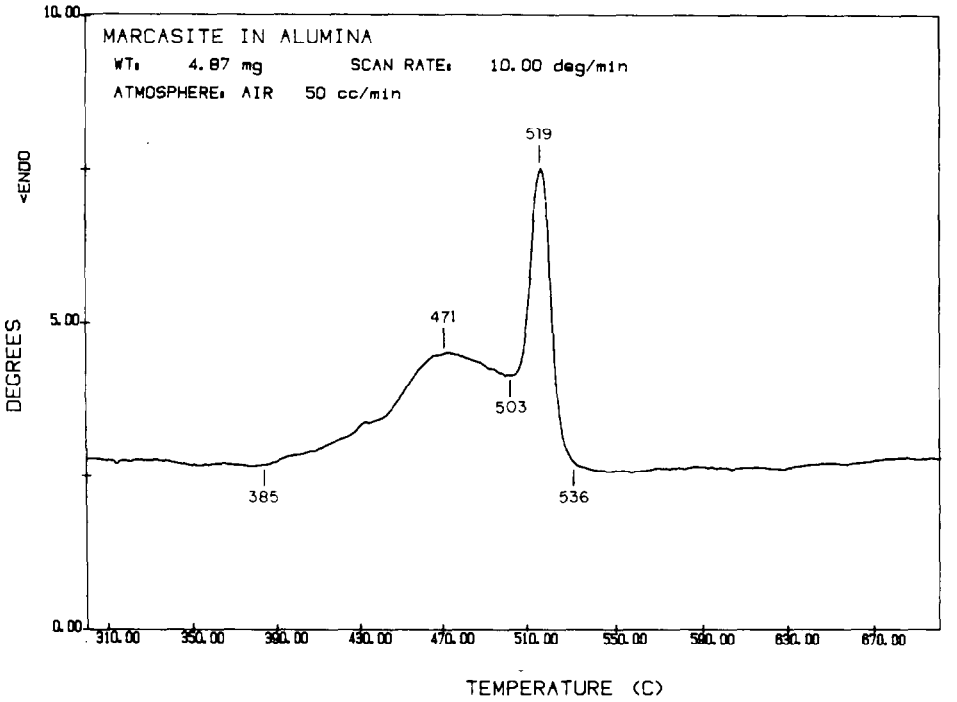

Fig. 6. DTA oxidative thermal curve of a marcasite/Al_2O_3 mixture containing 4.87 mg of marcasite.

Figure 6 shows the DTA curve obtained for a LTA specimen of the Herrin 6 seam (southwestern Illinois). This LTA specimen was analyzed to contain 9.9% total sulfur and the pyrite and marcasite content was estimated by XRD techniques to be 19 and 2%, respectively. Since this coal was subjected to low temperature ashing near 100°C in an oxygen plasma, the presence of considerable iron sulfates is likely. This is found to be the case, as is described in ref. 14 following this communication. Frazier and Belcher [15] reported that 25–75% of the pyrite in a set of Australian coals was affected by the LTA process. Rao and Gluskoter [16] have determined the iron sulfate content of 44 specimens from the Herrin 6 seam by XRD techniques. Their results showed that the iron sulfate content varied from 0 to 32%. In general, however, the iron sulfate minerals rarely comprised more than 7% of the LTA mineral matter for the Herrin 6 specimens.

The multistep exotherm, shown in Fig. 7, having relative minima and maxima at 407, 439, 464 and 508°C is associated with the pyrite oxidation in the presence of iron sulfates and other components in the LTA material. The endothermic peaks at 108 and 150°C are from the loss of interlayer water from both illite and illite–smectite clay mineral components of the LTA material. On comparing this thermal curve with that given in Figs. 1–5, a somewhat lower oxidative onset temperature (ca. 350°C) in the LTA and a lowering of the temperatures of the exothermic activity in general are noted.

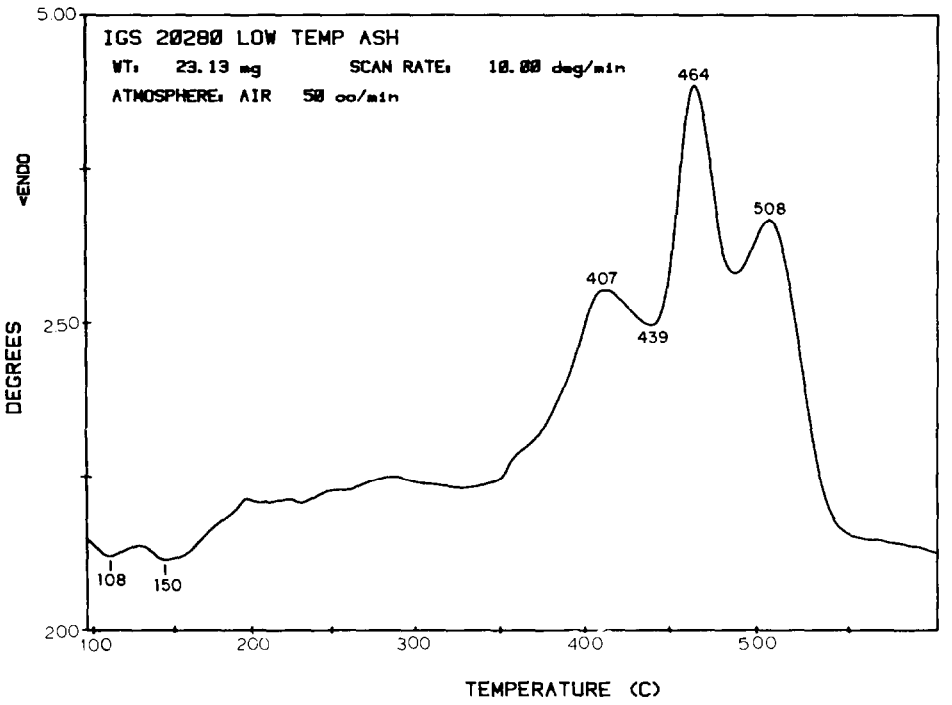

Fig. 7. DTA thermal curve for low temperature ash component of the Herrin 6 seam (southwestern Illinois) in dynamic air atmosphere.

Pyrite / iron sulfate / Al_2O_3 synthetic mixture

Since the LTA material is known to contain iron sulfates, from DTA and TG studies in other atmospheres as well as from XRD, a synthetic mixture containing 23.1% pyrite ore, 13.76% $FeSO_4 \cdot H_2O$, and 63.1% Al_2O_3 diluent was prepared. These levels of pyrite and iron sulfate were chosen since they were believed to be reasonable estimates of that in the LTA of the Herrin 6 seam. Figure 8 gives the DTA, TG, and DTG curves for this synthetic mixture. Although not labeled on the DTA curve, the exothermic region gives maxima at 465 and 520°C with a relative minima separating these at 478°C. The endotherm beginning near 600°C is the normal ferrous sulfate decomposition as observed in dynamic air purge [17]. When this DTA pattern is compared with that observed in Fig. 4 for the pyrite/Al_2O_3 mixture, one will note that the presence of iron sulfates lowers the temperature of the major peak maximum by 27°C and also converts the oxidative profile to a clearly defined two-stage event.

On comparing the DTA oxidative profile with the TG/DTG curves given in Fig. 8, it can be seen that the smallest exotherm at $T_{max} = 465$°C is associated with a weight gain while the second exothermic step is associated with weight loss. The two peaks observed in the pyrite/$FeSO_4 \cdot H_2O$ mixture

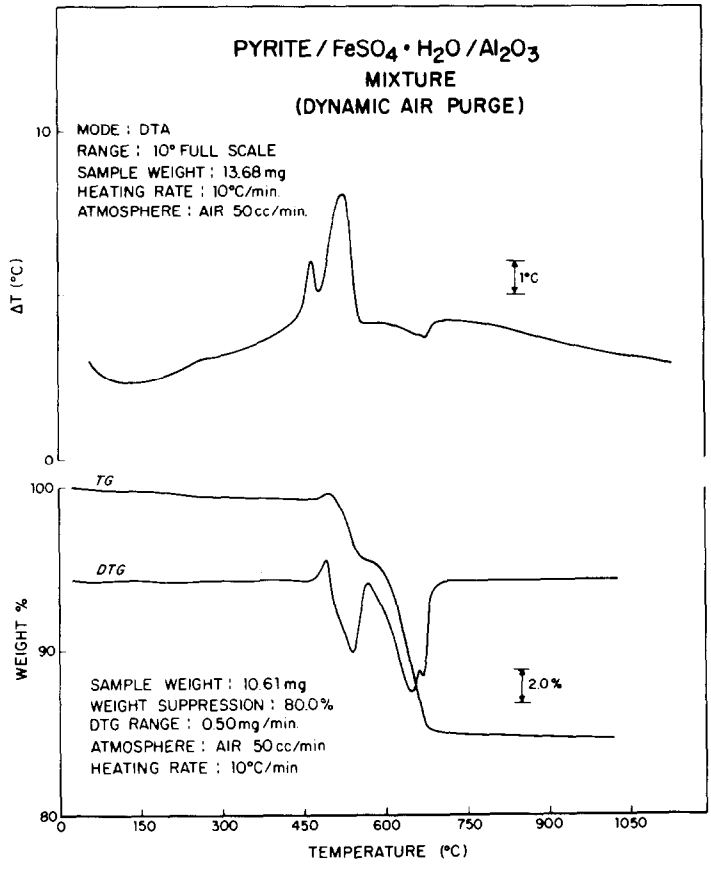

Fig. 8. DTA, TG, and DTG thermal curves for a pyrite/$FeSO_4 \cdot H_2O$/Al_2O_3 mixture in dynamic air atmosphere.

are in the same temperature region as the last two exothermic peaks in the LTA specimen of Fig. 6. Although agreement in peak temperature is observed in one case (i.e., 465°C in the synthetic mixture and 464°C in the LTA material), it is sometimes difficult to strictly identify thermal events in this fashion since the peak maximum varies with quantity or amount. This means that the exothermic peak maximum at 508°C in the LTA specimen could be the same as that in the pyrite/iron sulfate mixture at 520°C except in smaller quantity. It should be noted that the pyrite/iron sulfate synthetic mixture exhibits an iron sulfate decomposition above 600°C while the thermal curves for the pyrite/Al_2O_3 mixture did not.

Variation of the pyrite exothermic response with pyrite level in LTA specimens

A study was performed to see how the oxidative profile varied with the pyrite level in a series of LTA ash specimens. For this study, LTA specimens

TABLE 1

Pyrite and total sulfur content for the four LTA specimens of this study

LTA specimen	Pyrite (XRD estimate)(%)	% Total sulfur
Herrin 6	19	9.9
Hazard 7	2	1.7
Hazard 7A	5	3.8
Hazard 8	NA	6.5

NA = not analyzed.

from the Herrin 6 seam (southwestern Illinois), Hazard 8 seam (eastern Kentucky), and two specimens of the Hazard 7 seam from two different locations in eastern Kentucky were taken. Table 1 gives the estimated pyrite levels for three of the four LTA specimens as obtained by XRD techniques. The total sulfur, as assigned by the Perkin-Elmer 240C Elemental Analyzer, is also given for the LTA specimens. As can be seen, the pyrite level varies from as high as 19% in the Herrin 6 specimen to as low as 2% in the Hazard 7 LTA specimen.

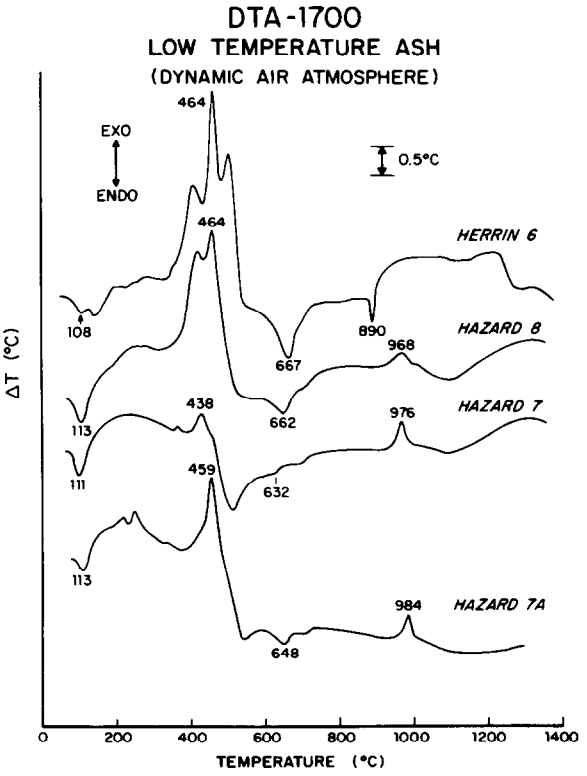

Fig. 9. Comparative DTA oxidative thermal curves for low temperature ash specimens of several pyrite containing coals.

Figure 9 shows the DTA oxidative thermal curves obtained for these LTA specimens in a dynamic air purge of 50 cm^3 min^{-1}. The sample weights used were 23.1 mg of the Herrin 6, 35.0 mg of the Hazard 8, 29.5 mg of the Hazard 7, and 28.7 mg of the Hazard 7A LTA specimen. The middle exothermic event ($T_{max} = 464°C$) in the Herrin 6 specimen is in common with the other three specimens; this event is observed at 464°C in the Hazard 8 LTA specimen, at 459°C in the Hazard 7A specimen, and at 465°C in the synthetic pyrite/$FeSO_4$ mixture. The temperature of this peak maxima decreases as the amount of pyrite decreases and thus occurs at 438°C for the Hazard 7 specimen which was estimated to contain only 2% pyrite.

From these thermal curves it might be predicted that the exothermic oxidative profiles become multipeaked and show activity at higher temperatures as the pyrite level increases. This is in agreement with the experiments given earlier in this work. The temperature of onset of oxidation is very similar in all four of the LTA specimens even though the mineral content of the Illinois coal is quite different from the three Kentucky coal LTA specimens. All four LTA specimens contained a significant iron sulfate component. This iron sulfate level being less as the pyrite level decreases; this may be seen by the decrease in magnitude and temperature of the decomposition peak observed at 667°C in the Herrin 6, 662°C in the Hazard 8, etc. This endothermic peak, in some cases, overlaps and predominates over less intense illite–smectite or smectite clay mineral dehydroxylation in these low temperature ash specimens.

The clay mineralogy was noticeably different in the four LTA specimens. For example, all three of the Kentucky coals contained detectable levels of kaolinite, as is evidenced by the exothermic ordering peak (spinel formation) at 968, 976, and 984°C in the Hazard 8, Hazard 7, and Hazard 7A, respectively. The Herrin 6 seam showed no evidence of kaolinite at the level of detectability of DTA. The double endothermic peak at 108 and 150°C in the Herrin 6 specimen is due to the loss of interlayer water from both illite and illite–smectite mixed layer clay minerals. The lower temperature event (108°C) may also be due, in part, to the dehydration of iron sulfate species such as the $FeSO_4 \cdot 7\ H_2O$ (melanterite), $FeSO_4 \cdot 4\ H_2O$ (rozenite), and $Fe_2(SO_4)_3 \cdot 9\ H_2O$ (coquimbite). The endothermic peaks in the Hazard 8 (113°C), Hazard 7 (111°C), and Hazard 7A (113°C) specimens also are due to the same water loss phenomenon. Because of the fact that the Hazard 7 specimen contains very little iron sulfate component, the thermal curves for the three Kentucky specimens indicate that these endothermic events are mostly due to the presence of illite and mixed layer clays containing illite clay mineral.

The Herrin 6 contained a measurable calcite component while the three Kentucky specimens did not. The endothermic peak at 890°C in the DTA thermal curve for the Herrin 6 seam is associated with the decomposition of

calcite although it is sharpened by its association with the oxidation products of the pyrite. This will be discussed in detail in a following paper [14]. It is also noted that the clay mineral dehydroxylation endotherm (ca. 540°C) which is observed immediately after the pyrite oxidation is more distinguishable in the Hazard 7 and 7A specimens than in the Hazard 8 specimen. This is primarily due to the lower kaolinite and higher pyrite levels in this specimen as compared to the two Hazard 7 specimens.

CONCLUSION

The temperature range as well as the nature of the exothermic oxidative profile for pyrite was found to be highly dependent upon sample size and heating rate. Smaller sample sizes and slower heating rates favor a more singular oxidative profile. Dilution of the pyrite or marcasite specimen with alumina or inert material allows a better oxidant availability to the sample material and more closely simulates the distribution of pyrite in natural specimens such as LTA specimens from coals.

The presence of iron sulfates lowers the peak temperature and converts the oxidative profile to a two-stage event. Furthermore, pyrite specimens, as well as LTA specimens from coals, containing significant levels of iron sulfates were observed to exhibit a DTA endothermic event between 630 and 670°C which is characteristic for the decomposition/oxidation of the iron sulfate component. This thermal event was absent from the DTA oxidative thermal curves for pyrite samples which initially contained no iron sulfates.

The DTA oxidative profiles for LTA specimens containing varying amounts of pyrite and iron sulfates showed that the exothermic oxidation of the pyrite component becomes more multistep in nature as the pyrite level increases. The iron sulfate content of the LTA material was observed to increase with the pyrite in the same specimen. This was reflected in the DTA curves by the magnitude of the endothermic event near 660°C. In the LTA specimens of this study, this iron sulfate decomposition/oxidation endotherm near 660°C in the DTA curve was observed to overlap and, in some cases, masks the less intense endothermic dehydroxylation of mixed layer clays which contain smectite clay mineral components.

Those LTA specimens containing a significant amount of kaolinite clay mineral exhibited an endothermic (dehydroxylation) effect just above the pyrite oxidation peaks. Kaolinite was also easily recognized in the three Kentucky LTA specimens by the characteristic exothermic ordering peak at 970–1000°C. The loss of interlayer water from illite and illite–smectite mixed layer clay minerals seemed to predominate as endothermic events in the 100–150°C range of the DTA oxidative thermal curve. Calcite was observed in the Herrin 6 LTA specimen as an endothermic decomposition peak at 890°C. This peak is sharpened in the presence of large amounts of pyrite and iron sulfates.

ACKNOWLEDGMENTS

The author expresses his sincere appreciation to Ms. Faith L. Fiene for both the low temperature ash specimens and supporting XRD results. He also thanks Mr. R.F. Culmo and Kathy Weisgable for performing the sulfur analyses presented in this work.

REFERENCES

1 R.C. Mackenzie, The Differential Thermal Investigation of Clays, Mineralogical Society, London, 1957, p. 366.
2 J.R. Blachere, J. Am. Ceram. Soc., 49 (1966) 590.
3 L.G. Berg and E.N. Shlyapkina, J. Therm. Anal., 8 (1975) 329.
4 A.C. Banerjee, in W. Hemmenger (Ed.), Thermal Analysis ICTA 80, Vol. 2, Birkhaeuser Verlag, Basel, 1980, pp. 241–246.
5 N. Chakrabarti, D.R. Glasson and S.A.A. Jayaweera, Thermochim. Acta, 51 (1981) 77.
6 R. Dimitrov and B. Boyanov, Thermochim. Acta, 64 (1983) 27.
7 D.N. Todor, Thermal Analysis of Minerals, Abacus Press, Kent, 1976, pp. 116–117.
8 E.M. Bollin, in R.C. Mackenzie (Ed.), Differential Thermal Analysis, Vol 1, Academic Press, London, 1970, p. 193.
9 H.-J. Shyu, P.O. Vaishnava and P.A. Montano, Fuel, 60 (1981) 1022.
10 G.M. Schwab and J. Philinis, J. Am. Chem. Soc., 769 (1947) 2588.
11 O.C. Kopp and P.F. Kerr, Am. Mineral., 43 (1958) 1079.
12 R.A. Schloenlaub, J. Am. Ceram. Soc., 52 (1969) 40.
13 T. Kennedy and B.T. Sturman, J. Therm. Anal., 8 (1975) 329.
14 C.M. Earnest, in preparation.
15 F.W. Frazier and C.B. Belcher, Fuel, 52 (1973) 41.
16 C.P. Rao and H.J. Gluskoter, Occurrence and Distribution of Minerals in Illinois Coals, Illinois Geological Survey Circular 476, Urbana, Illinois, 1973.
17 P.K. Callagher, D.W. Johnson and F. Schrey, J. Am. Ceram. Soc., 53 (1970) 666.